

Electronic Supplementary Information

**Vibrational autoionization of state-selective jet-cooled methanethiol  
(CH<sub>3</sub>SH) investigated with infrared + vacuum-ultraviolet  
photoionization**

Min Xie,<sup>a</sup> Zhitao Shen,<sup>a</sup> S. T. Pratt<sup>\*b</sup> and Yuan-Pern Lee<sup>\*ac</sup>

<sup>a</sup> *Department of Applied Chemistry and Institute of Molecular Science, National  
Chiao Tung University, Hsinchu 30010, Taiwan. Email: [yplee@mail.nctu.edu.tw](mailto:yplee@mail.nctu.edu.tw);  
Tel: +886-3-5131459*

<sup>b</sup> *Argonne National Laboratory, Argonne, Illinois 60439, USA. Email: [stpratt@anl.gov](mailto:stpratt@anl.gov)*

<sup>c</sup> *Institute of Atomic and Molecular Sciences, Academia Sinica, Taipei 10617,  
Taiwan*

## Table of Contents

**Table S1.** Observed and fitted term values of Rydberg series in Fig. 2(a).

**Table S2.** Selected Franck-Condon factors (FCF) between the normal modes of CH<sub>3</sub>SH and CH<sub>3</sub>SH<sup>+</sup> calculated with the B3LYP/aug-cc-pVDZ method.

**Table S3.** Observed and fitted term values of Rydberg series in Fig 2(b).

**Table S4.** Observed and fitted term values of Rydberg series in Fig. 3.

**Table S5.** Observed and fitted term values of Rydberg series in Fig. 4(a)

**Table S6.** Observed and fitted term values of Rydberg series in Fig. 4(b)

**Figure S1.** Single-photon VUV photoionization efficiency (VUV-PIE) spectrum of CH<sub>3</sub>SH in the range 75600–77600 cm<sup>-1</sup>.

**Figure S2.** First-derivative plots of the PIE curves in Fig. 2.

**Figure S3.** First-derivative plot of the PIE curve in Fig. 3.

**Figure S4.** First-derivative plots of the PIE curves in Fig. 4.

**Table S1.** Observed term values of Rydberg series in Fig. 2(a) and corresponding fitted values according to Eq. (2). The spectrum was obtained by fixing the IR laser at  $2601\text{ cm}^{-1}$  ( $\nu_3$  mode of  $\text{CH}_3\text{SH}$ ) while scanning the VUV laser. The principal quantum number is  $n$ , the quantum defect is  $\delta$ , and the fitted converging energy is  $\text{IE}_v$

$n$	$(ns \leftarrow 3a'')$			$(np \leftarrow 3a'')$			$(nd \leftarrow 3a'')$			$(nf \leftarrow 3a'')$		
	Obs.	Individual fitting <sup>a</sup>	Global fitting <sup>b</sup>	obs.	Individual fitting <sup>a</sup>	Global fitting <sup>b</sup>	obs.	Individual fitting <sup>a</sup>	Global fitting <sup>b</sup>	obs.	Individual fitting <sup>a</sup>	Global fitting <sup>b</sup>
7	--	74175		--	75106		76302	76303	76301	76545	76548	76545
8	--	75601		--	76152		76904	76905	76902	77067	77067	77065
9	76455	76452	76455	76809	76807	76809	77307	77310	77309	77422	77423	77422
10	77005	77001	77003	77239	77244	77243	77592	77596	77595	77675	77678	77678
11	77378	77375	77379	77555	77550	77549	77808	77806	77806	77862	77867	77867
12	77650	77642	77646	77772	77773	77771	77967	77964	77963	78013	78011	78011
13	77844	77839	77844	77939	77940	77937	78086	78086	78086	78124	78123	78123
14	77992	77988	77993		78068			78183		78213	78212	78212
15		78104			78169			78260		78284	78283	78284
16		78195			78250			78323		78339	78342	78343
$\text{IE}_v$		$78770 \pm 2$	$78770 \pm 1$		$78774 \pm 5$	$78770 \pm 1$		$78770 \pm 2$	$78770 \pm 1$		$78769 \pm 1$	$78770 \pm 1$
$\delta$		$2.11 \pm 0.01$	$2.12 \pm 0.01$		$1.53 \pm 0.01$	$1.52 \pm 0.01$		$0.33 \pm 0.01$	$0.33 \pm 0.01$		$-0.03 \pm 0.01$	$-0.02 \pm 0.01$

<sup>a</sup> Fitted for each individual series. <sup>b</sup> Simultaneous fitting of all series using the same  $\text{IE}_v$ .

**Table S2.** Selected Franck-Condon factors (FCF) between the normal modes of CH<sub>3</sub>SH and CH<sub>3</sub>SH<sup>+</sup> calculated with the B3LYP/aug-cc-pVQZ method. FCF including the Duschinsky effect were calculated using the harmonic approximation with the ezSpectrum v3.0 program

ionic \ neutral	assignment	0	$\nu_1$	$\nu_2$	$\nu_3$	$\nu_9$	$2\nu_4$	$2\nu_{10}$
0 <sup>+</sup>		<b>0.6290</b>	0.0011	0.0028	0.0059	0.0000	0.0009	0.0004
$\nu_1^+$	CH <sub>3</sub> stretch (a')	0.0005	<b>0.5859</b>	0.0408	0.0000	0.0000	0.0000	0.0000
$\nu_2^+$	CH <sub>3</sub> stretch (a')	0.0049	0.0386	<b>0.5793</b>	0.0001	0.0000	0.0000	0.0000
$\nu_3^+$	SH stretch (a')	0.0062	0.0000	0.0002	<b>0.6166</b>	0.0000	0.0000	0.0000
$\nu_4^+$	CH <sub>2</sub> scissor (a')	0.0242	0.0017	0.0005	0.0004	0.0000	0.0163	0.0000
$\nu_5^+$	CH <sub>3</sub> deform (a')	0.0104	0.0004	0.0001	0.0001	0.0000	0.0072	0.0000
$\nu_6^+$	CH <sub>3</sub> rock (a')	0.0592	0.0005	0.0020	0.0008	0.0000	0.0000	0.0000
$\nu_7^+$	SH bend (a')	0.0188	0.0000	0.0013	0.0000	0.0000	0.0000	0.0000
$\nu_8^+$	CS stretch (a')	0.1446	0.0001	0.0003	0.0015	0.0000	0.0000	0.0001
$\nu_9^+$	CH <sub>2</sub> stretch (a'')	0.0000	0.0000	0.0000	0.0000	<b>0.6214</b>	0.0000	0.0000
$\nu_{10}^+$	CH <sub>3</sub> rock (a'')	0.0000	0.0000	0.0000	0.0000	0.0007	0.0000	0.0000
$\nu_{11}^+$	CH <sub>3</sub> deform (a'')	0.0000	0.0000	0.0000	0.0000	0.0001	0.0000	0.0000
$\nu_{12}^+$	CS torsion (a'')	0.0000	0.0000	0.0000	0.0000	0.0034	0.0000	0.0000
$2\nu_4^+$		0.0003	0.0001	0.0000	0.0000	0.0000	<b>0.4052</b>	0.0000
$2\nu_{10}^+$		0.0001	0.0000	0.0000	0.0000	0.0000	0.0000	<b>0.6036</b>

<sup>a</sup> $\nu_i$  and  $\nu_i^+$  denote the  $i$ -th vibrational modes of neutral and cationic CH<sub>3</sub>SH, respectively;  $\nu_1$ : symmetric CH<sub>2</sub> stretch,  $\nu_2$ : symmetric CH<sub>3</sub> stretch,  $\nu_3$ : S-H stretch,  $\nu_9$ : antisymmetric CH<sub>2</sub> stretch,  $2\nu_4$ : overtone of CH<sub>2</sub> scissor,  $2\nu_{10}$ : overtone of CH<sub>3</sub> rock; 0 and 0<sup>+</sup> indicate vibrational ground states of neutral and cationic CH<sub>3</sub>SH, respectively.

**Table S3.** Observed term values of Rydberg series in Fig. 2(b) and corresponding fitted values according to Eq. (2). The spectrum was obtained by fixing the IR laser at  $2948 \text{ cm}^{-1}$  ( $\nu_2$  mode of  $\text{CH}_3\text{SH}$ ) while scanning the VUV laser. The principal quantum number is  $n$ , the quantum defect is  $\delta$ , and the fitted converging energy is  $\text{IE}_v$

$n$	$(ns \leftarrow 3a'')$			$(np \leftarrow 3a'')$			$(nd \leftarrow 3a'')$		
	Obs.	Individual fitting <sup>a</sup>	Global fitting <sup>b</sup>	Obs.	Individual fitting <sup>a</sup>	Global fitting <sup>b</sup>	Obs.	Individual fitting <sup>a</sup>	Global fitting <sup>b</sup>
7	--	74533		--	75419		76662	76657	76659
8	--	75967		76490	76487	76490	77262	77263	77263
9	76823	76823	76826	77156	77153	77153	77676	77671	77673
10	77379	77374	77374	77597	77597	77597	77957	77960	77961
11	77751	77749	77749	77909	77907	77907	78173	78171	78173
12	78015	78017	78017	78130	78132	78132	78332	78330	78332
13	78216	78214	78214	78304	78301	78301		78452	
14	78363	78364	78363		78431			78549	
$\text{IE}_v$		$79141 \pm 2$	$79140 \pm 1$		$79141 \pm 2$	$79140 \pm 1$		$79138 \pm 3$	$79140 \pm 1$
$\delta$		$2.12 \pm 0.01$	$2.11 \pm 0.01$		$1.57 \pm 0.01$	$1.56 \pm 0.01$		$0.35 \pm 0.01$	$0.35 \pm 0.01$

<sup>a</sup> Fitted for each individual series. <sup>b</sup> Simultaneous fitting of all series using the same  $\text{IE}_v$ .

**Table S4.** Observed term values of Rydberg series in Fig. 3 and corresponding fitted values according to Eq. (2). The spectrum was obtained by fixing the IR laser at  $3014\text{ cm}^{-1}$  (overlapped  $\nu_1$  and  $\nu_9$  modes of  $\text{CH}_3\text{SH}$ ) while scanning the VUV laser. The principal quantum number is  $n$ , the quantum defect is  $\delta$ , and the fitted converging energy is  $\text{IE}_v$ .

$n$	$(ns \leftarrow 3a'')$			$(np \leftarrow 3a'')$			$(nd \leftarrow 3a'')$		
	Obs.	Individual fitting <sup>a</sup>	Global fitting <sup>b</sup>	Obs.	Individual fitting <sup>a</sup>	Global fitting <sup>b</sup>	Obs.	Individual fitting <sup>a</sup>	Global fitting <sup>b</sup>
Ionization to $\text{CH}_3\text{SH}^+$ ( $\nu_1$ )									
7	--	74684		--	75580 <sup>c</sup>		76811	76811	76813
8	--	76118		76644	76642		77422	77417	77419
9	76970	76974	76971		77306		77824	77825	77826
10	77522	77525	77523		77748		78117	78114	78114
11	77902	77900	77899		78057		78324	78325	78325
12	78168	78168	78167		78281		78481	78484	78484
13	78363	78365	78364		78450			78606	
14	78513	78515	78514		78579			78703	
$\text{IE}_v$		$79292 \pm 2$	$79291 \pm 1$		79288			$79292 \pm 2$	$79291 \pm 1$
$\delta$		$2.12 \pm 0.01$	$2.12 \pm 0.01$		1.56			$0.35 \pm 0.01$	$0.35 \pm 0.01$
Ionization to $\text{CH}_3\text{SH}^+$ ( $\nu_9$ )									
7	--	74584		--	75522		76720	76719	76723
8	--	76018		76569	76568	76566	77328	77323	77325
9	76876	76874	76876	77222	77222	77223	77735	77730	77730
10	77426	77425	77426	77655	77659	77660	78012	78017	78017
11	77802	77800	77801	77964	77965	77967	78228	78227	78227
12	78067	78068	78068	78193	78188	78190	78387	78386	78385
13	78267	78265	78265		78355			78508	
14	78415	78415	78415		78483			78605	
$\text{IE}_v$		$79192 \pm 1$	$79192 \pm 2$		$79189 \pm 3$	$79192 \pm 2$		$79193 \pm 3$	$79192 \pm 2$
$\delta$		$2.12 \pm 0.01$	$2.12 \pm 0.01$		$1.53 \pm 0.01$	$1.56 \pm 0.01$		$0.34 \pm 0.01$	$0.33 \pm 0.01$

<sup>a</sup> Fitted for each individual series. <sup>b</sup> Simultaneous fitting of all series using the same  $\text{IE}_v$ . <sup>c</sup> Lines in this series were calculated using  $\text{IE} = 79288\text{ cm}^{-1}$  and  $\delta = 1.56$ .

**Table S5.** Observed term values of Rydberg series in Fig. 4(a) and corresponding fitted values according to Eq. (2). The spectrum was obtained by fixing the IR laser at  $2867\text{ cm}^{-1}$  ( $2\nu_{10}$  mode of  $\text{CH}_3\text{SH}$ ) while scanning the VUV laser. The principal quantum number is  $n$ , the quantum defect is  $\delta$ , and the fitted converging energy is  $\text{IE}_v$ .

$n$	$(ns \leftarrow 3a'')$			$(np \leftarrow 3a'')$			$(nd \leftarrow 3a'')$		
	Obs.	Individual fitting <sup>a</sup>	Global fitting <sup>b</sup>	Obs.	Individual fitting <sup>a</sup>	Global fitting <sup>b</sup>	Obs.	Individual fitting <sup>a</sup>	Global fitting <sup>b</sup>
7	--	74387		--	75292		--	76530	
8	--	75821		--	76353		77130	77132	77132
9	76676	76677	76677	--	77016		77539	77537	77536
10	77228	77228	77226	77459	77457	77459	77825	77824	77824
11	77606	77603	77603	77766	77766	77767	78031	78033	78032
12	77872	77871	77871	77995	77991	78991	78195	78191	78191
13	78071	78068	78068	78152	78159	78159	78310	78313	78312
14	78216	78218	78218	78293	78288	78288	78407	78410	78409
15	78331	78334	78333	78390	78390	78389	78489	78487	78486
16	78428	78425	78426	78469	78471	78470		78550	
17	78503	78499	78500	78540	78537	78536		78602	
18	78557	78560	78560		78591			78646	
19	78608	78610	78610		78636			78682	
20	78648	78652	78652		78674			78713	
$\text{IE}_v$		$78995 \pm 1$	$78995 \pm 1$		$78997 \pm 3$	$78995 \pm 1$		$78997 \pm 2$	$78995 \pm 1$
$\delta$		$2.12 \pm 0.01$	$2.12 \pm 0.01$		$1.56 \pm 0.01$	$1.55 \pm 0.01$		$0.33 \pm 0.01$	$0.33 \pm 0.01$

<sup>a</sup> Fitted for each individual series. <sup>b</sup> Simultaneous fitting of all series using the same  $\text{IE}_v$ .

**Table S6.** Observed term values of Rydberg series in Fig. 4(b) and corresponding fitted values according to Eq. (2). The spectrum was obtained by fixing the IR laser at  $2892\text{ cm}^{-1}$  ( $2\nu_4$  mode of  $\text{CH}_3\text{SH}$ ) while scanning the VUV laser. The principal quantum number is  $n$ , the quantum defect is  $\delta$ , and the fitted converging energy is  $\text{IE}_v$ .

$n$	$(ns \leftarrow 3a'')$			$(np \leftarrow 3a'')$			$(nd \leftarrow 3a'')$		
	Obs.	Individual fitting <sup>a</sup>	Global fitting <sup>b</sup>	Obs.	Individual fitting <sup>a</sup>	Global fitting <sup>b</sup>	Obs.	Individual fitting <sup>a</sup>	Global fitting <sup>b</sup>
7	--	74439		--	75390		--	76520	
8	--	75865		--	76426		77144	77143	77143
9	--	76716		77073	77075	77075	77556	77556	77556
10	77265	77265	77265	77511	77509	77508	77842	77847	77846
11	77643	77640	77640	77813	77813	77812	78056	78060	78058
12	77908	77906	77907	78031	78034	78033	78220	78220	78219
13	78103	78103	78104	78199	78200	78199	78349	78344	78342
14	78248	78252	78253	78328	78328	78327		78441	
15	78370	78368	78369		78428			78520	
$\text{IE}_v$		$79028 \pm 3$	$79030 \pm 2$		$79031 \pm 2$	$79030 \pm 2$		$79033 \pm 3$	$79030 \pm 2$
$\delta$		$2.11 \pm 0.01$	$2.11 \pm 0.01$		$1.51 \pm 0.01$	$1.51 \pm 0.01$		$0.38 \pm 0.01$	$0.38 \pm 0.01$

<sup>a</sup> Fitted for each individual series. <sup>b</sup> Simultaneous fitting of all series using the same  $IE_v$ .

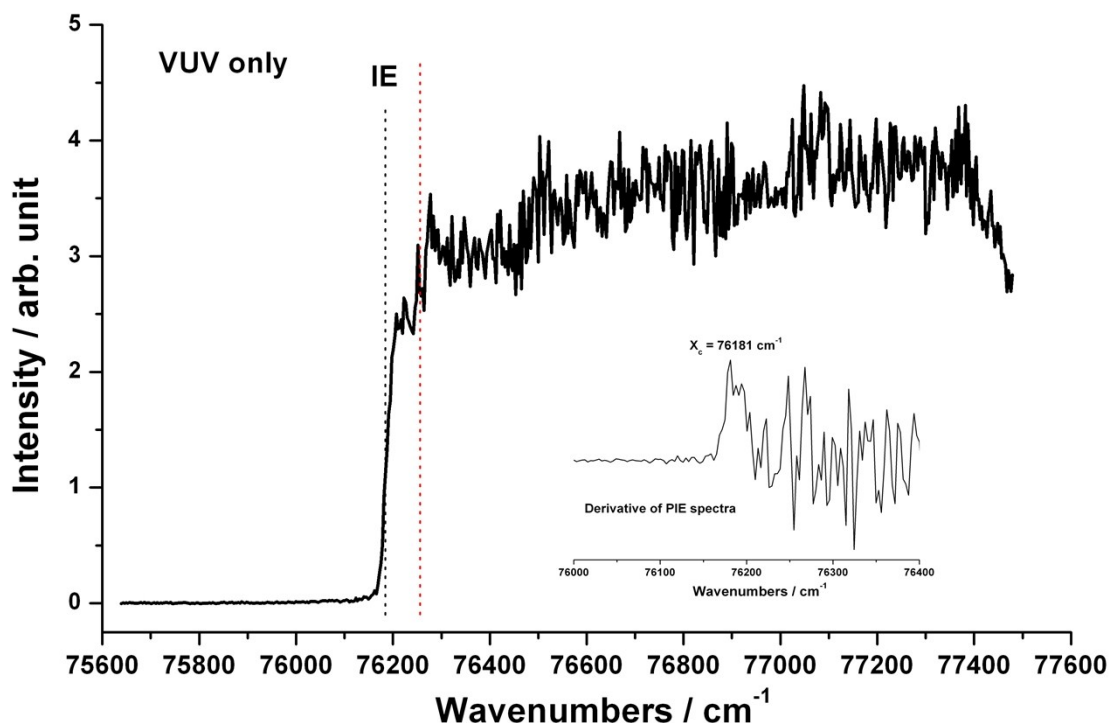


**Fig. S1.** Single-photon VUV photoionization efficiency (VUV-PIE) spectrum of  $\text{CH}_3\text{SH}$  in the range  $75600\text{--}77600\text{ cm}^{-1}$ . The position marked with the black dotted line (at  $76181\text{ cm}^{-1}$ ) is the maxima of the first-order derivative of the PIE spectrum (shown in the inset). The ionization threshold (IE) of  $\text{CH}_3\text{SH}$ ,  $76256.3 \pm 2.9\text{ cm}^{-1}$ , reported by Cheung *et al.* (J. Chem. Phys. 1998, **109**, 1781) is indicated with a red dotted line. The difference between these two values is due to the shift induced by the electric field. The single step and absence of resonant structure indicates the Franck-Condon factors between the ground state neutral and cation are nearly diagonal, that is, that the potential surfaces of the two states are very similar near their equilibrium geometries.

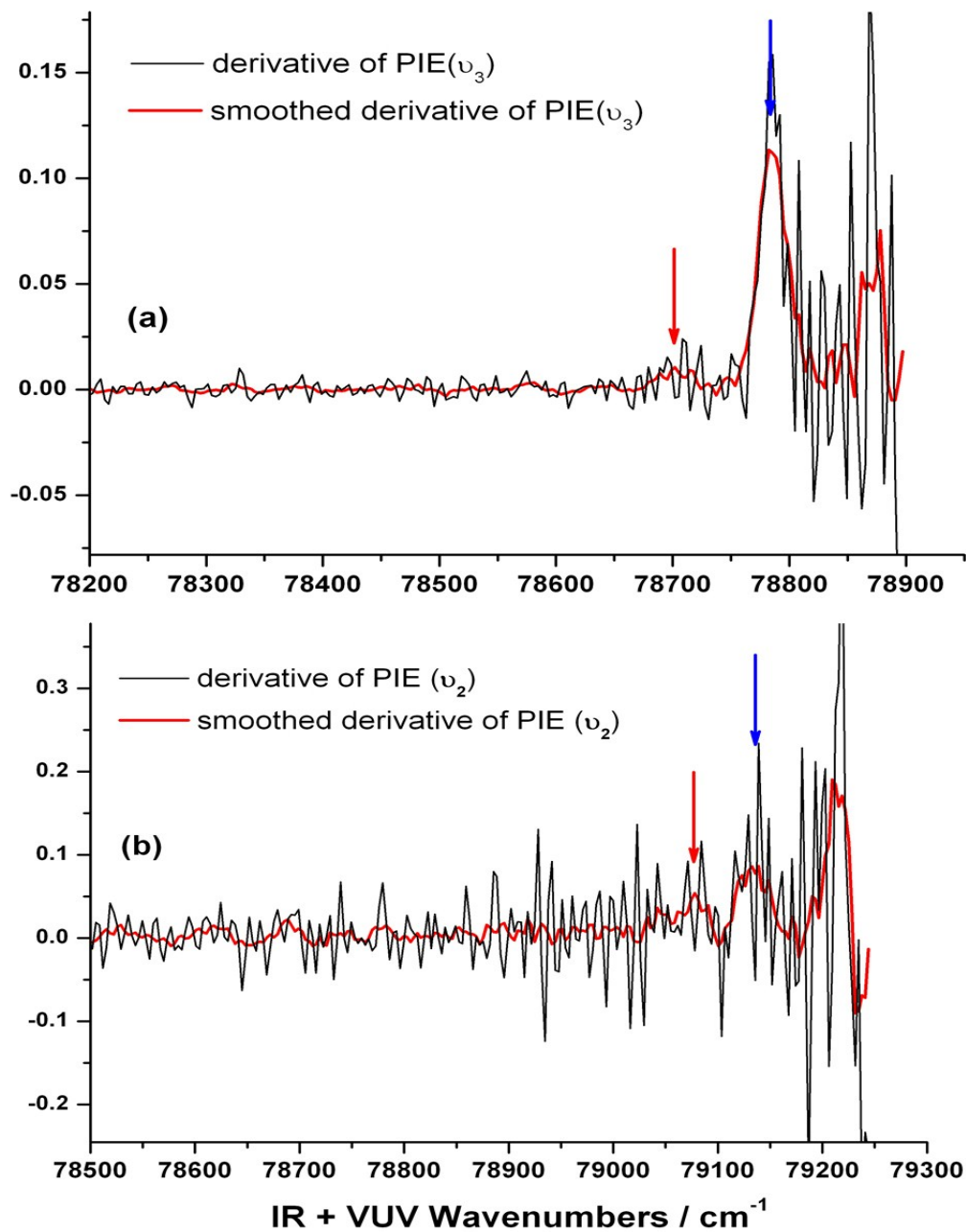


**Fig. S2.** The first-order derivative of the photoionization efficiency (PIE) curves in Fig. 2. The first two maxima, marked with the red and blue arrows, respectively, indicate the step positions.

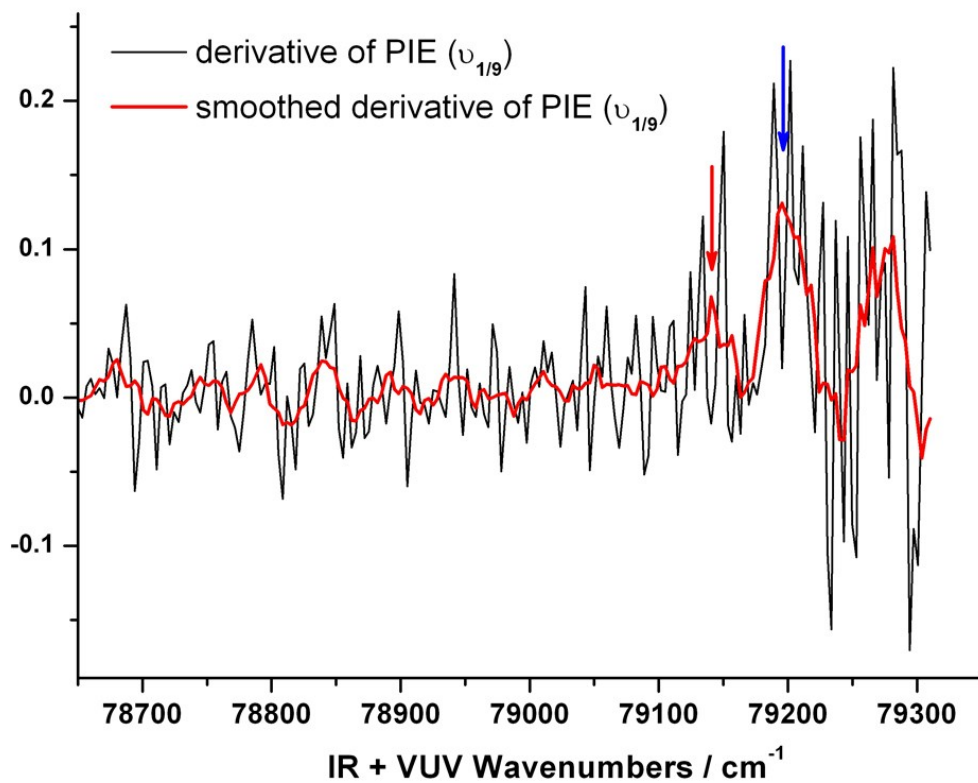


**Fig. S3.** The first-order derivative of the photoionization efficiency (PIE) curves in Fig. 3. The first two maxima, marked with the red and blue arrows, respectively, indicate the step positions.

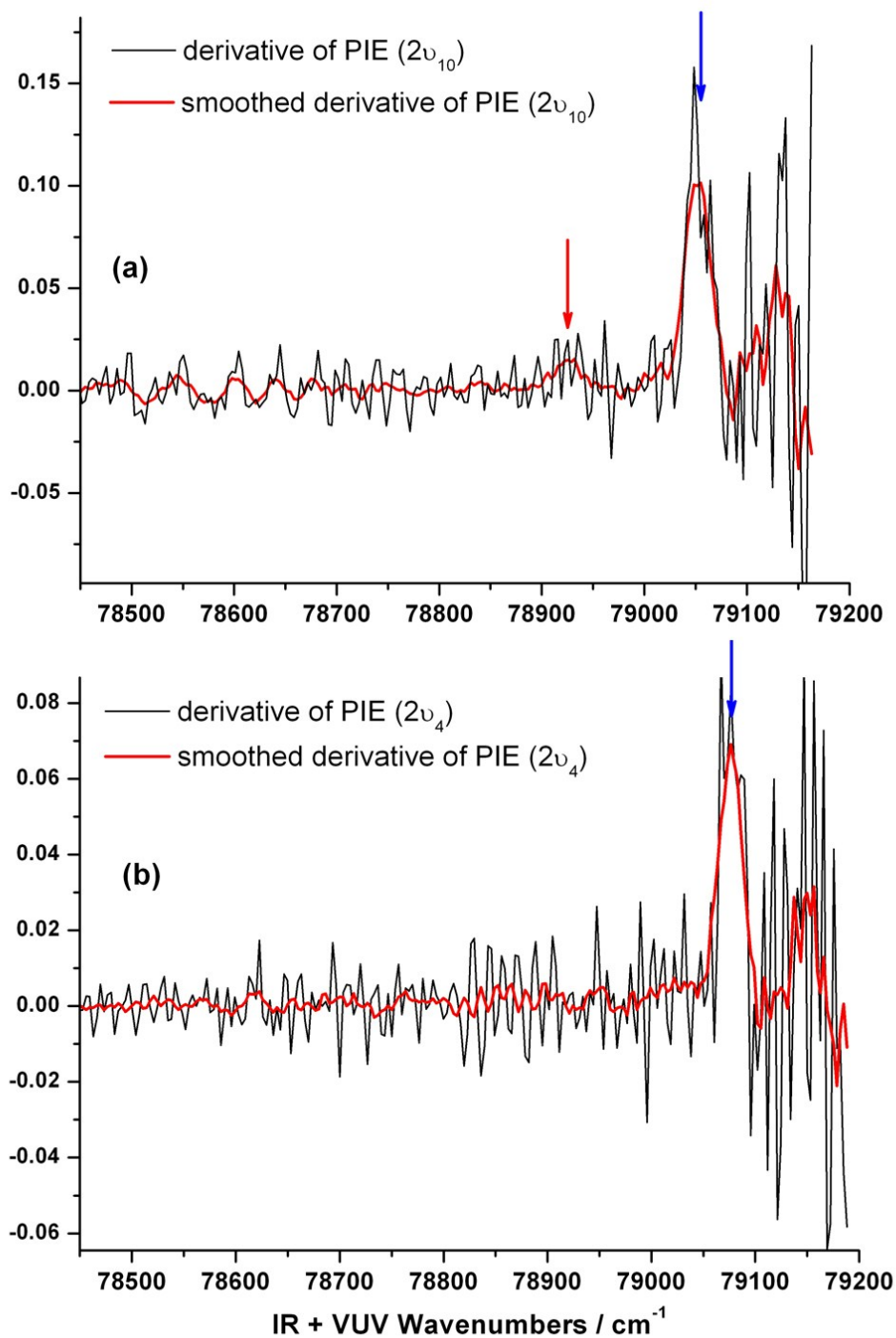


**Fig. S4.** The first-order derivative of the photoionization efficiency (PIE) curves in Fig. 4. The first two maxima, marked with the red and blue arrows, respectively, indicate the step positions. For (b) only one step could be clearly identified.